The final publication is available at

http://doi.org/10.1002/polb.24564

Additional Information

Crystallization kinetics of poly(ethylene oxide) confined in semicrystalline poly(vinylidene) fluoride

Maria N. Tamaño-Machiavello[1], Carlos M. Costa[2], Francisco J. Romero-Colomer[1], José María Meseguer Dueñas[1,3], Senentxu Lanceros-Mendez[4,5], José Luis Gómez Ribelles[1,3]

[1]Centre for Biomaterials and Tissue Engineering (CBIT), Universitat Politècnica de València, Camino de Vera s/n, 46022 Valencia, Spain.
[2]Centro de Física, Universidade do Minho, 4710-057 Braga, Portugal
[3]Biomedical Research Networking Center in Bioengineering, Biomaterials and Nanomedicine (CIBER-BBN), Valencia, Spain.
[4]BCMaterials, Parque Científico y Tecnológico de Bizkaia, 48160-Derio, Spain
[5]IKERBASQUE, Basque Foundation for Science, 48013, Bilbao, Spain.

Correspondence to: C. M. Costa (E-mail: *cmscosta@fisica.uminho.pt*)

((Additional Supporting Information may be found in the online version of this article.))

ABSTRACT

Polymer blends based on poly(vinylidene fluoride), PVDF, and poly(ethylene oxide), PEO, have been prepared in order to analyze the crystallization kinetics of poly(ethylene oxide) confined in semicrystalline PVDF with different ratios of both polymers. Both blend components were dissolved in a common solvent, dimethyl formamide. Blend films were obtained by casting from the solution at 70 ºC. Thus, PVDF crystals are formed by crystallization from the solution while PEO (which is in the liquid state during the whole process) is confined between PVDF crystallites. The kinetics of crystallization of the confined PEO phase was studied by isothermal and non-isothermal experiments. Fitting of Avrami model to the experimental DSC traces allows a quantitative comparison of the influence of the PVDF/PEO ratio in the blend on the crystallization behavior. The effect of melting and further recrystallization of the PVDF matrix on PEO confinement is also studied.

KEYWORDS: Electroactive polymers; crystallization; confinement

INTRODUCTION

There has been much interest in understanding the effect of physical confinement on polymer crystallization. Polymer droplets, thin layers, or filling the pores of other polymers or ceramics can be considered physical confinement systems in which even if the interaction between the polymer chains and the confinement material can be more or less intense, no chemical bonding hinders polymer segments diffusion. The effect of confinement on crystallization kinetics comes from different factors such as the change in nucleation mechanisms, the limitation to crystal growth or the dependence of melting temperature on crystal volume [1,2]. Crystallization in melt miscible polymer blends is also affected by the change of the diffusion of the polymer chains to the crystal growth surface, while crystallization of a component of a block copolymer is affected by all these confinement factors but in addition to the limitation of chain segments diffusion due to the connectivity between blocks in the copolymer chains [3].

In the particular case of poly(ethylene oxide), PEO, crystallization kinetics has been studied in many different confinement systems. Micro or nano- layers confined between rigid polymeric layers leads to a strong decrease of the crystallization rate when layer thickness decreases from micro to nano-scale [4,5]. Thousands of polymer nanolayers were obtained with a layer-multiplying coextrusion process and it was shown that layers with thickness in the order of 20 nm leads to PEO crystallization as single, high-aspect-ratio lamellae that resemble single crystals [6]. Further, the relaxation behavior was observed to depend on layer thickness in [7]. PEO was also confined by infiltration within alumina nanopores, showing that within pores with a volume of around 10^{-8} mm^3 PEO crystallizes solely via homogeneous nucleation [8], leading to a significant reduction of the crystallization temperature [9]. On the other hand, crystallization of PEO in blends or copolymers have been studied: melt miscible crystalline-amorphous blends [10-12], miscible crystalline-crystalline blends [13], in immiscible blends [14],

block copolymers [15,16] and electrospun nanofibers of ternary blends containing PEO were also studied, the crystallization behavior of PEO being dependent on the composition of the system that significantly affected crystal nucleation [17].

A comparison of different confinement geometries was presented in [18] and the effect of the elastic properties of confinement medium was analyzed in [19]. Some general trends can be deduced of the analysis of the experimental data comparing the crystallization kinetics of bulk PEO with that of confined PEO, such as the decrease of the Avrami exponent and the crystallization rate with confinement, as well as the decrease of crystallization temperature in non-isothermal crystallization on cooling. Nevertheless, the data obtained present large differences in the different works probably due to differences in average molecular weight of the polymer, presence of impurities that could act as surfaces for heterogeneous nucleation and different thermal histories, among others.

In our recent paper [20] poly(vinylidene fluoride)/poly(ethylene oxide), PVDF/PEO crystalline-crystalline blends were prepared with a procedure that confines PEO chains between PVDF crystalline entities. A similar procedure was used previously to confine PEO in poly(vinylidene fluoride-co-trifluoroethylene) copolymers [21-25]. Briefly, a solution of both components in dimethyl formamide, DMF, was homogenized and solvent allowed to slowly evaporate at 70 ºC. At this temperature PVDF crystallizes from the solution while PEO chains are in the liquid state up to the end of the drying process since PEO melting temperature is below 70 ºC. Then on cooling to room temperature PEO crystallizes confined by the existing PVDF crystals.

Recently, a deep study on the miscibility and crystallization kinetics of PVDF/PEO blends has been reported [26], concluded that the two components are miscible in the liquid state from the changes in the crystallization kinetics of each component in the blend with respect to the corresponding homopolymer. Crystallization on cooling produces phase separation with

micrometric domains of PVDF or PEO rich phases.

The two-step crystallization procedure from the solution, proposed in references [20-25], allowed obtaining a very homogeneous dispersion of PEO in a matrix formed by the piezoelectric polymer. The understanding of the physical properties of the water absorbing PEO rich phase of the blend is essential for the application of these blends in areas of increasing interest such as sensors and actuators [27], filtration membranes [28] and battery separator membranes [29]. The dispersion of PEO polymer chains among PVDF crystals is so fine that microscopy techniques do not allow a complete picture of the microstructure of the blend. Some insight into the blend microstructure was obtained in reference [20] by extracting the PEO phase from the blend by washing the blend membranes in water. Nevertheless, some membrane contraction occurs indicating that small changes in PVDF microstructure could take place while extracting PEO phase. In this work a further insight is obtained on PEO chain mobility in this blend by following the crystallization process induced by different thermal treatments in which PVDF crystals are not expected to suffer any transformation, since the maximum temperature of the experiments is well below the melting temperature of PVDF. As the results show, crystallization of PEO in the blends of this work is very different to that of PEO in PVDF/PEO blends crystallized from the melt, as reported in reference [26]. Interestingly the effect of the proximity of PVDF crystals on PEO crystallization rate can be just the opposite in our system crystallized in two steps from the solution than in that crystallized from the melt. It is worth noting that polarized optical microscopy cannot be used to follow crystal growth [30] due to the high dispersion of the PEO domains within the sample, thus, our study is based on calorimetric experiments that reveal the ability of PEO chains reorganization even in very small confined domains.

EXPERIMENTAL

Materials and polymer blends preparations

PVDF (Mw 700000 g/mol) and PEO (Mw 100000 g/mol) were acquired from Solvay and Polysciences, respectively. PVDF/PEO blends were prepared with compositions of 70/30, 50/50 and 0/100 weight ratios. Blends were prepared by dissolving the adequate amounts of both polymers in N,N-dimethylformamide (DMF) at a 15/85 w/v polymer / solvent ratio. The polymers were dissolved at 80 ºC for 48 hours with the help of a magnetic stirrer in a glass vessel with outer jacket for the circulation of water until a homogeneous and transparent solution could be observed. The solutions were deposited in Petri dishes and the solvent was allowed to evaporate at 70 ºC for two hours. Finally, complete removal of the solvent was achieved in vacuum for another 3 hours at 70 ºC.

Characterization techniques

To observe phase morphology through scanning electron microscopy (SEM) images, PEO was removed by immersion in water for up to 7 days, while the water was changed every day. After 7 days, the samples were dried in open air and subsequently in vacuum at 40 °C for one day. The microstructure of the blend films were examined in a field emission scanning electron microscope (FESEM), ZEISS Ultra-55, after the deposition of a conductive layer of sputtered platinum. A series of samples were observed after melting a blend film at 200 ºC in an oven on a glass sheet.

Differential scanning calorimetry (DSC) analysis was carried out with a Perkin-Elmer DSC 8000 instrument under a flowing nitrogen atmosphere. Cooling and heating thermograms were recorded between 25 and 200 ºC at a heating rate of 20 ºC min^{-1}. For isothermal crystallization experiments, samples were heated to 90 ºC for 5 minutes and cooled down to the crystallization temperature at the highest cooling rate at which the DSC is kept under control during the whole cooling scan: 80 ºC/min. A series of experiments were performed

also in the same conditions but after melting PVDF in the sample pan by heating at 200 ºC for 5 minutes and then cooling down to 100 ºC at 20 ºC min⁻¹. All samples were measured in 30 µL aluminum pans with perforated lids to allow the release and removal of volatiles. The isothermal crystallization was analyzed by origin plug software [31].

RESULTS AND DISCUSSION

Morphology

The microstructure of the PVDF/PEO blend was analyzed by FESEM. This is the most suitable characterization method considering the sample preparation conditions used in the present work, in which PEO chains are pushed by the growing PVDF crystals that crystallizes from the solution during solvent evaporation. Thus, PEO remains confined in spaces between PVDF spherulites or in interlamelar spaces mixed with amorphous PVDF chains [20]. In order to reveal the details of the sizes of PEO domains and PVDF-PEO interface, PEO was extracted from the blend by washing in water at room temperature. The hydrophobicity of PVDF justifies the expectation that the PVDF phase remains unaltered while PEO is extracted from the blend. Figure 1 shows the microstructure of the surface of 50/50 and 70/30 blends after PEO extraction.
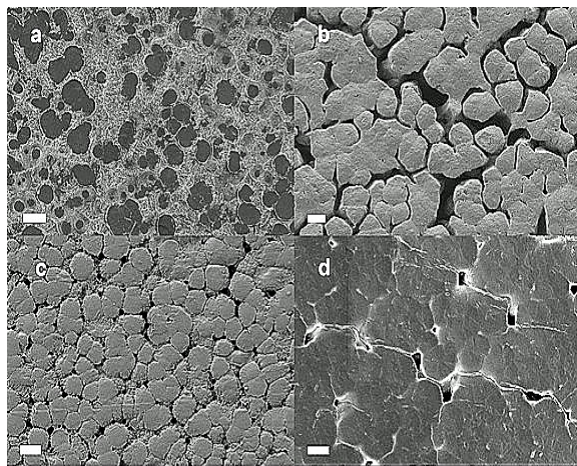

FIGURE 1 FESEM pictures of the surface of PVDF/PEO blend samples produced by

crystallization of PVDF while casting from the solution in DMF at 70ºC (a) 50/50 (c) 70/30 sample. The images (b) and (d) correspond to the same samples after melting PVDF at 200ºC and recrystallization on cooling from the melt. Dimension bar 10 microns.

The shape of PVDF spherulites formed during crystallization from the solution in DMF appears clearly in the 70/30 sample. In the case of 50/50 sample the spherulites that appears at the surface are more separated from each other while a continuous layer of rough material appears among them. This structure is clearer in the view of the cross section of the sample (Figure 2): the shape of the spherulites can be clearly observed in the 70/30 sample, touching each other leaving free spaces between them that should be occupied by PEO before the extraction in water.
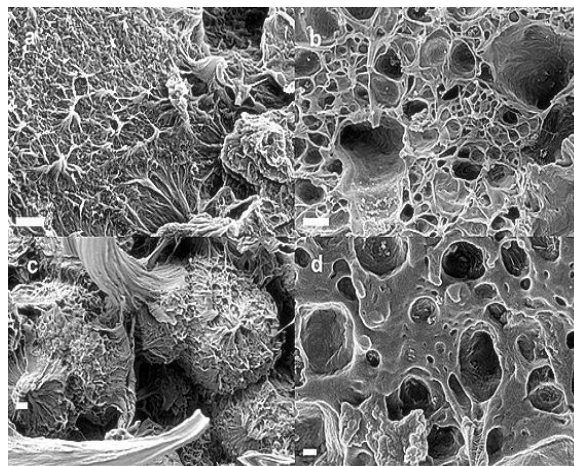

FIGURE 2 As in Figure 1, but the cross-section of the cryo-fractured samples is shown in the FESEM pictures. Dimension bar 1 micron.

Nevertheless, in the 50/50 blend the cross-section shows a continuous phase with no free volume, indicating that PVDF may collapse during PEO extraction. This fact was discussed in more detail in [20]. After melting of both PVDF and PEO by annealing the samples at 200 ºC and recrystallizing on cooling from the melt, the phase morphology changes mainly in the 50/50

sample showing a sharper separation between the two components. Now, the space occupied by PEO before extraction and the spherulite growth of the PVDF crystals is more apparent. In reference [26], indications of miscibility of PVDF and PEO in the molten blend were obtained from crystallization kinetics. Thus, the change of microstructure on melting and recrystallization is expected to take place due to the segregation of the toe phases during crystallization from the melt. The change of microstructure is more apparent in the cross-section, at the higher magnification of Figure 2. The spherulite diameters are between 7 and 10 μm either in the 50/50 or in the 70/30 blends. The pictures of Figure 1 show that after PVDF crystallization, a fraction of PEO is placed in the interspherulitic regions of PVDF whose dimensions are in the order of one micron in the 70/30 blend and in the order of few microns in the 50/50 blend. On the other hand, the roughness of the PVDF surfaces remaining after PEO extraction informs about the topology of the interface between PVDF and confined PEO.

Isothermal crystallization

Figure 3 shows representative plots of the DSC traces during isothermal crystallization of bulk and confined PEO. Experiments were conducted up to 200 minutes but only the first 10 min interval in which the traces are more significant is presented. Crystallization rate first increases as the undercooling increases, as it can be seen in Figure 3a for the sample 50/50 at 30 ºC, where the maximum of the exotherm appears just 20 seconds after reaching the crystallization temperature. Experiments at lower temperatures are considered unrealistic with our calorimeter since a significant crystallization would take place during the cooling scan. On the other hand, the experimental temperature interval was limited at high crystallization temperatures by the long crystallization times required to reach equilibrium. The peak in the heat flow plot of Figure 3b (corresponding to the maximum crystallization rate, as shown in equation (4)) is clearly shifted towards shorter

times in the 50/50 sample with respect to bulk PEO. Acceleration of the crystallization kinetics of PEO in the blends due to the nucleating effect of PVDF surfaces was already reported in reference [26]. Nevertheless, for the 70/30 sample the peak corresponding to the maximum crystallization rate it is much shifted towards times longer than 1000 s, and does not appear in the time interval of Figure 3b.
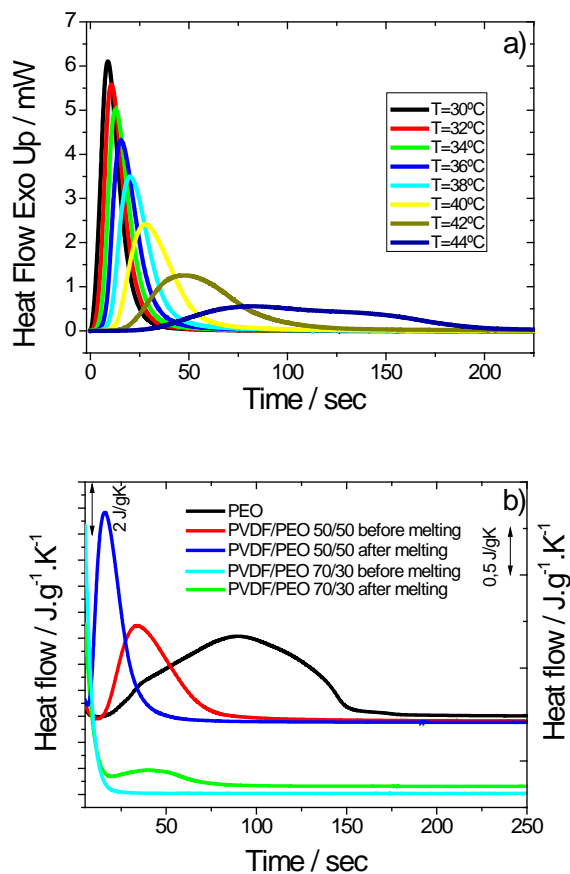

FIGURE 3 a) Isothermal crystallization of the 50/50 sample at different temperatures before the melting of PVDF phase. (b) DSC isotherms for the crystallization at 40 ºC of bulk PEO and PEO in 50/50 and 70/30 samples before and after melting of PVDF phase. Note the change of scale for 70/30 blend (right axis). The exothermic peak in the 70/30 sample before melting of the PVDF phase appears at this temperature at times above 1000 s and it is not shown in the plot.

This trend is further confirmed by the half-time crystallization time, $t_{1/2}$, shown in Figure 4a).

Calculation of $t_{1/2}$ cannot be performed in the case of the 70/30 sample before melting of PVDF phase for temperatures higher than 35 °C because the long-time side of the peak is not well defined, and determination of the baseline for integration is not accurate enough.
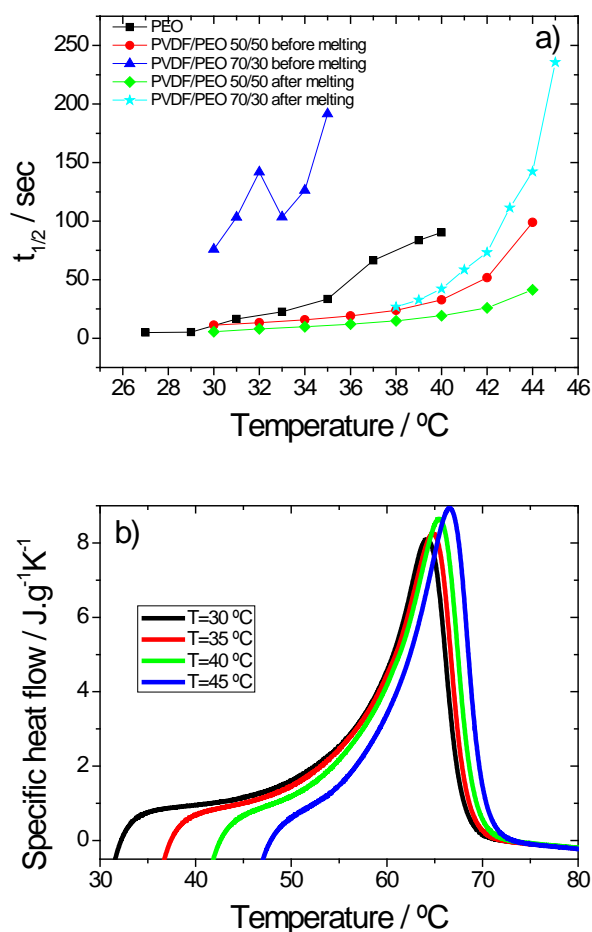

FIGURE 4 a) half-time crystallization ($t_{1/2}$) as a function of crystallization temperature for all samples and b) heating peak after isothermal crystallization at different temperatures for the 50/50 sample before the melting of the PVDF phase.

Figure 4b) shows the heating behavior after isothermal crystallization at different temperatures for the 50/50 sample before the melting of the PVDF phase. As expected, heating

after isothermal crystallization shows a melting peak, the temperature of the maximum of the endotherm increasing with increasing crystallization temperature, indicating an increase of crystal thickness with crystallization temperature. The behavior is similar for confined and non-confined PEO crystals

The PEO crystalline fraction at time t, Xct, was calculated by integration of the heat flow thermograms. The maximum crystalline fraction at temperature T when the sample equilibrates was determined as

$$X_\infty(T) = \frac{1}{w_{PEO}} \frac{\Delta H_\infty}{\Delta H_f^0} \qquad (1)$$

Where ΔH_∞ is the enthalpy increment calculated by integration of the heat flow curve, ΔH_f^0 is the heat of melting of the PEO single crystal taken as ΔH_f^0 = 203 J.g^{-1} [32], and w_{PEO} is the weight fraction of PEO in the blend. The baseline for integration was determined at times well above the crystallization exotherm, when the experimental heat flow is stable, and extrapolated to the whole thermogram.

The maximum crystallinity attained during isothermal crystallization is approximately the same in bulk PEO and in the 50/50 sample: around 70%, whereas in the 70/30 sample the fraction of PEO able to crystallize is just between 5 and 8%. Thus, it can be said that confinement of PEO between the crystallites of PVDF is so strong that most of the PEO chains are unable to diffuse and incorporate to the growing crystals. On the other hand, the kinetics of crystallization of the PEO fraction able to crystallize is much retarded with respect to bulk PEO.

The experimental results can be fitted to Avrami equation [33,34]

$$\frac{X_{ct}}{X_{c\infty}(T)} = 1 - \exp(-Kt^n) \qquad (2)$$

Where n is the Avrami's exponent related to the geometry of crystal growth, the nucleation mechanism and how the rate of incorporation of a polymer chain to growing crystal is controlled [35,36], and K is the rate constant. The fit has been usually performed by linearizing equation (2) to give

$$\log\left[-\ln\left(1-\frac{X_{cy}}{X_{c\infty}(T)}\right)\right] = \log K + n\log t \quad (3)$$

The plot of the left side of equation (3) against log t allows determining n and K. Deviation from linearity are observed frequently at high conversion, which is ascribed to the start of secondary relaxation, a change in the geometry of crystal growth [5] or a change in the nucleation mechanism in the sense of the Lauritzen-Hofman theory [37-39].

Nevertheless, fitting of the experimental isotherms to equation (3) can be carried out by direct non-linear least squares fitting and the interval in which the results cannot be predicted by the model can be observed directly in the original diagrams. To do that, the heat flow delivered by the sample according to equation (2) is calculated by [40]:

$$\dot{q}(t) = X_{c\infty}(T)\frac{\rho_c}{\rho}\Delta H_f^0\frac{dX_c}{dt} \quad (4)$$

where $\dot{q}(t)$ is the heat flow emitted by the sample at time t, ρ and ρ_c are the density of the semicrystalline PEO and that of the crystal phase, respectively.

The crystalline mass fraction $\left(\dfrac{X_{ct}}{X_{c\infty}(T)}\right)$ was converted to relative volumetric fraction taking into account the fully crystalline and fully amorphous polymer densities of the PEO polymer [31] as it is illustrated in the Avrami plot for each sample (figure 5).

Figure 5 shows the comparison of the experimental data of bulk PEO and the model equation at two crystallization temperatures, the insets show the double logarithmic plot according to equation (3).
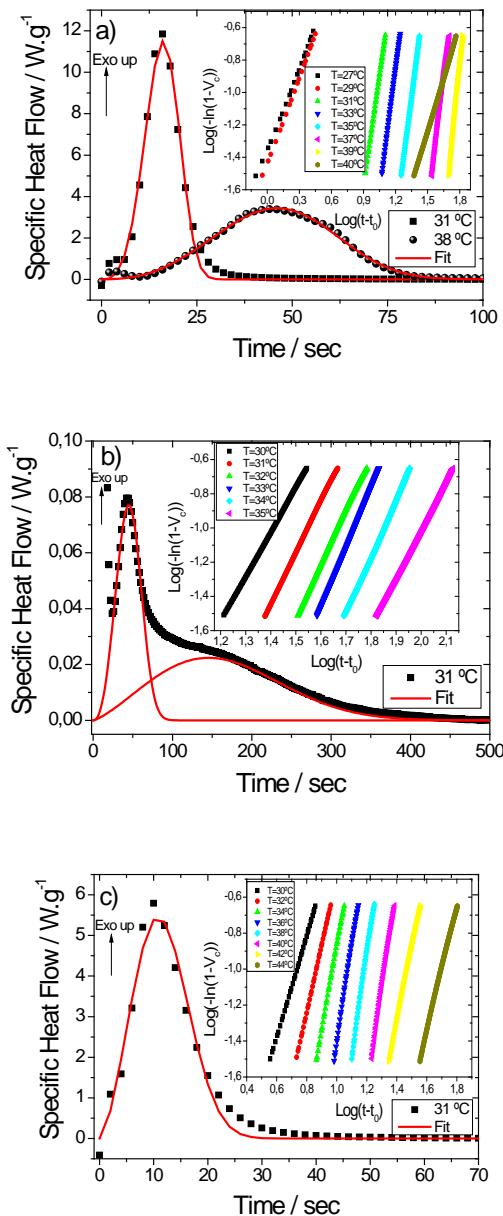

FIGURE 5 Isothermal crystallization at 31ºC with the corresponding fitting for PEO (a), 70/30 (b) and 50/50 (c) samples before melting of the PVDF phase. The 38 ºC isotherm for PEO is also

included in Figure (a). The Avrami plot for each sample is shown in the insets.

The Avrami equation can be well adjusted to the experimental results at low conversions for all the samples. In bulk PEO only small differences between the experiment and the model are detected at low crystallization temperatures in the high conversion side of the heat flow plot. The impossibility of Avrami equation to fit the shape of the heat flow diagram in the high conversion side is more apparent in the confined samples, as shown in Figure 5b and 5c. In the case of 70/30 blend the experimental results show a fractionated crystallization [1] that can be explained by the presence of several nucleation mechanisms in different regions or by limiting conditions to crystal growth by confinement in regions small enough to modify crystal size and orientation. In the case of 70/30 sample the fitting process was conducted with the sum of two Avrami processes.

The values of the Avrami exponent and rate constant are listed in Table 1 for the different crystallization temperatures. Avrami exponent for bulk PEO depends on the crystallization temperature with values between 3 and 4.3. The results found in the literature cover the range between 1 and 4.5. It seems that very low values are found for high molecular weight polymers [41], other authors report values bellow 2.5 [4,5,10,11,42-45], while values above 3 were found in other references [15,26,46]. It is not unexpected the lack of reproducibility of crystallization kinetics in a given polymer since it is highly influenced on the one hand by the nucleation process that is highly dependent on the presence of impurities and the contact with external surfaces and, on the other hand, on the characteristics of the polymer chain such as molecular weight distribution or the presence of chain defects. The theoretical value of n=4 is predicted for spherical growth and homogeneous nucleation with crystal growth controlled by the attachment of the polymer chains to the crystal surface [15,35,36]. In the confined systems, Avrami exponent decreases. In the case of the 70/30 blend, in the fraction

that crystallizes faster n takes values between 3.2 and 3.5 while n= 2.3 for the high conversion side of the plot that would correspond to the slow crystallization rate fraction. A clear decrease of Avrami exponent has been found in polymers physically confined in different confinement geometries [1,4,5] and it is ascribed to the change in nucleation mechanism and in crystal growth geometry, in some cases with crystal alignment.

TABLE 1 Parameters for isothermal crystallization of bulk PEO and PEO in 50/50 and 70/30 samples before and after melting of the PVDF phase

Sample	T / ºC	n	Ln K
PEO	30	3.6	-9.74
	32	3.7	-11.30
	34	3.9	-13.11
	36	4.4	-16.02
	38	3.4	-13.30
	40	2.8	-13.09
50/50 before melting of PVDF	30	2.4	-6.03
	32	2.8	-7.30
	34	3.0	-8.52
	36	3.2	-9.70
	38	3.4	-10.49
	40	3.4	-11.91
50/50 after melting of PVDF	30	1.8	-3.28
	32	2.2	-4.84
	34	2.6	-6.11
	36	2.9	-7.43
	38	3.1	-8.57

	40	3.2	-9.66
	30	3.2, 2.3 (2° peak)	-11.68, -7.53 (2° peak)
70/30 before melting of PVDF	32	3.4, 2.3 (2° peak)	-14.17, 12.02 (2° peak)
	34	3.5	-16.67
	35	3.4	-18.16
	38	2.2	-7.53
70/30 after melting of PVDF	40	2.4	-9.41
	42	2.6	-11.43
	44	2.7	-13.83

A comparison of the rate constant of the confined and bulk PEO is prevented by the dependence of K units with the exponent n.

Non-Isothermal crystallization

The cooling thermograms recorded at different cooling rates are shown in Figure 6. It is shown that the crystallization temperature range becomes broader and it shifts to lower temperatures with increasing cooling rate as it is demonstrated in figure 6 for all samples. The temperature for half crystallization $T_{1/2}$ on cooling and the total crystalline fraction obtained at low temperatures are represented in Figure 7.
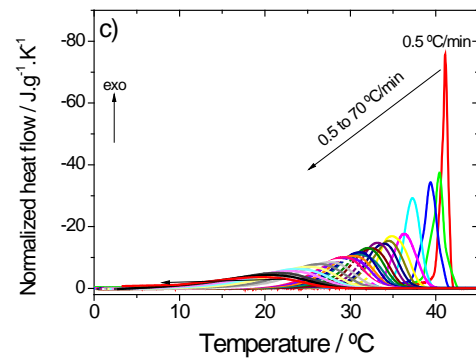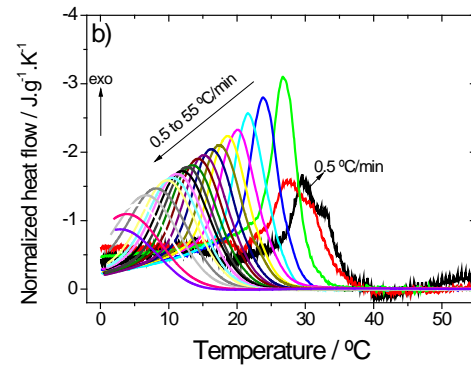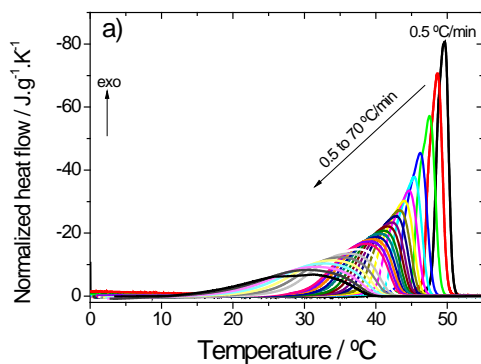

FIGURE 6 Normalized heat flow as a function of temperature at different cooling rates for PEO (a) and before melting of PVDF for 70/30 (b) and 50/50 (c).
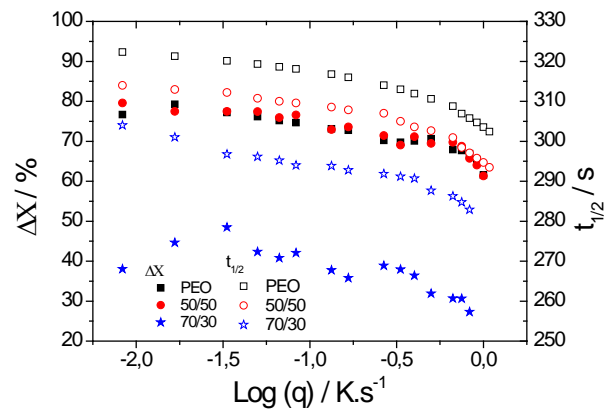

FIGURE 7 Degree of crystallinity and half-time of crystallization ($t_{1/2}$) as a function of the cooling rate for the samples before melting of PVDF phase.

Confinement produces an important shift of the crystallization peaks towards lower temperatures. In the case of 70/30 blend confinement reduces the half-time of crystallization and the temperature of the exothermic peak by 25ºC with respect to bulk PEO. In this sample, the presence of a long tail of crystallization at low temperatures seems consistent with the fractionation of crystallization observed in the isothermal measurements. Interestingly enough, the results for the 50/50 blend show a clear decrease of 6 ºC in $T_{1/2}$ towards lower temperatures with respect to bulk PEO, in spite that in isothermal crystallization it was shown that the crystallization rate slightly increased in this sample as can be seen in Figure 5. It is worth noting the different crystallization behavior in the 50/50 blend, while in isothermal experiments acceleration of the crystallization process is clear and can be ascribed to an enhanced nucleation of PEO in the interphases with PVDF crystals, nucleation process in a cooling ramp can be very different to that taking place after a temperature jump since nucleation rate is highly temperature-dependent. In this case the crystallization peak is shifted towards lower temperatures in the cooling ramps. It seems that in this case the limitation to crystal growth imposed by confinement is the main factor determining the rate of growth of the crystal mass.

The treatment of these kind of results with crystallization models is conceptually complex. The model of Ozawa [47] has been used in to describe the non-isothermal crystallization of PEO [42,46,48,49]. The Avrami model has been applied to crystallization on cooling by a conversion of the temperature to time scales [46,49,50]. And also a combination of Avrami and Ozawa methods has been proposed [48,51-54].

Actually, it can be said that there is no model able to reproduce the result of non-isothermal experiments from the isothermal crystallization data [49]. That requires the assumption of an additivity rule. If a given thermal history, starting a T_0 in the molten state, is simulated by a series of temperature steps followed by isothermal annealing leading to the same average temperature vs. time dependence, additivity would mean that the total crystalline fraction attained at time t would be the sum of the crystalline fraction increments in every previous isothermal annealing. But this requires to assume that the evolution of the crystallization process after a temperature step to temperature T_i, X_{i0} depends only on the crystal fraction of the sample at that moment and is independent on the previous thermal history. In particular the evolution during the annealing at T_i should be the same that after a temperature jump from T_0 to T_i followed by the crystallization time required to reach the crystallinity X_{i0}. This behavior is hardly found since nucleation is highly sensitive to thermal history and the number of nuclei could be very different after slow cooling or after a temperature step. Avrami pointed that additivity would be met in isokinetic conditions i.e. if the nucleation rate is proportional to crystal growth rate [34,55]. In the case of PEO crystallization, Addonizio et al [56] found that additivity correctly reproduced non-isothermal crystallization results, while Ozawa model did not.

To test additivity with our experimental results, cooling rates were simulated by a series of temperature jumps followed by isothermal stages to give the average experimental cooling rate.

$$\frac{X_{ct}}{X_{c\infty}(T)} = 1 - \exp\left(-K_m t^m\right) \quad (5)$$

The pre-exponential factor and Avrami exponent K_m and m respectively are in principle considered to be different from those obtained from the isothermal experiments. And the temperature dependence of K_m was in the form of Lauritzen-Hofman theory

$$K_m(T) = A \exp\left(\frac{-B}{T - T_\infty}\right) \exp\left(\frac{-C}{T(T_m - T)}\right) \quad (6)$$

Where T_∞ is the temperature at which the relaxation time of the conformational

rearrangements diverge, usually accepted to be around 50 ºC below the glass transition temperature. Although different experimental techniques show that the difference between T_∞ and the glass transition temperature can vary significantly from polymer to polymer, it is not expected to change with blend composition and we will accept the value of 50ºC in order not to add a new fitting parameter in the model equations. T_m is the equilibrium melting temperature and A, B and C are constants.

A non-linear search routine allows determining m and K_m for the best simultaneous fit of the thermograms obtained on cooling at different cooling rates: 5, 16, 28, 40 and 60 ºC/min. The model parameters obtained are listed in Table 2 and model simulated curves are represented in Figure 8.

TABLE 2 Parameters obtained from equations (5) and (6)

		PVDF/PEO			
		Before melting of PVDF		After melting of PVDF	
	PEO	50-50	70-30	50-50	70-30
m	2.25	2.45	2.06	2.59	2.51
C	87.84	32.89	14.10	57.12	32.40
A	9381	2359.08	477.96	5499.93	3288.51
B	300000	300000	300000	300000	300000

Interestingly, the model is able to reproduce the thermograms obtained at high and low cooling rates with the same set of model parameters, but the value of the Avrami exponent m is ~2.5, significantly lower than the exponent n obtained from the isothermal scans. This fact was also encountered in other works fitting non-isothermal crystallization thermograms with Ozawa-Avrami or modified Avrami model [42,46,49,52]. Deviation at low cooling rates and at low temperatures (high conversions) can be observed in 50/50 blend (Figure 8b) and, as

expected from isothermal experiments, the fractionation of the crystallization process in 70/30 blend makes that model only reproduces the high temperature side of the thermograms. The exponent m slightly decreases with confinement as happened in the isothermal results, even if in the case of 70/30 blend, only the fit of the high temperature side of the exotherm is considered.
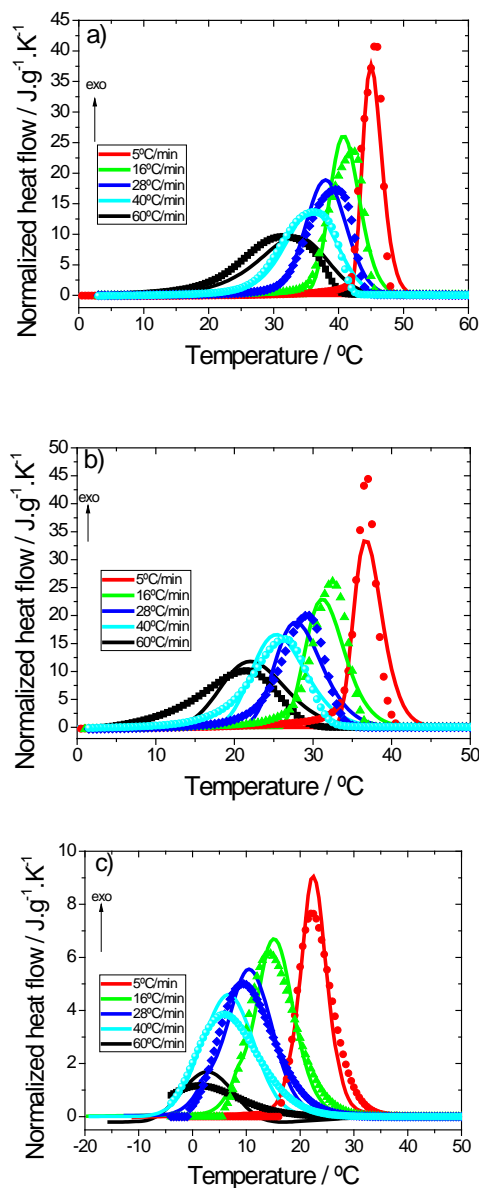
FIGURE 8 Cooling thermograms for PEO (a) and before melting of PVDF for 50/50 (b) and 70/30 (c) at different cooling rates.

PEO confined in melt crystallized PVDF

On melting and recrystallization of PVDF major morphological changes can be expected in the PVDF-PEO blend. Figure 1b and Figure1d show the SEM pictures of the surface of the 50/50 and 70/30 blends after subjecting them to a thermal treatment at 200ºC to melt PVDF, followed by cooling to room temperature. Figures 2b and 2d show the cross-section. It seems that segregation of the two components is more effective when PVDF crystallizes from the melt. After extracting PEO the cross-section images show the microstructure of the interface between PVDF and PEO, which presents smoother surfaces when PVDF crystallizes from the melt than from the solution in DMF. Nevertheless, PVDF and PEO highly interpenetrate in the micrometer scale. It seems that phase separation of the molten components precedes crystallization producing well defined interfaces.

The segregation of the PEO phase has a clear effect on PEO crystallization kinetics, as shown in the isothermal DSC traces of Figure 3. In the case of the 70/30 blend the crystallization enthalpy significantly increases (to around 26% in isothermal crystallization) what probes that an important fraction of the PEO chains that were confined between PVDF crystals when the later were formed from the solution, migrate to larger PEO domains when PVDF crystals melt. Maximum crystalline fraction attained in isothermal crystallization ranges between 20 and 25%. On the other hand, PEO crystallization becomes faster and Avrami exponent decreases in comparison to the values of pure PEO both from isothermal experiments or from cooling ramps (Table 1 and Table 2, respectively). This demonstrates a change in the nucleation mechanism and growth of PEO crystals when confined.

In the case of the 50/50 blend, the change in the Avrami coefficient or the maximum crystalline fraction obtained in isothermal crystallization experiments are not significant. Since PEO was already in domains large enough to allow crystallization, melting and recrystallization of PVDF phase seems to produce small changes in PEO behavior in this blend. The finding that in this blend

CONCLUSIONS

PVDF-PEO blends were produced by casting from a common solvent at a temperature above melting temperature of PEO. In this condition, the sample containing 50% PEO shows a crystallization rate and crystalline fraction similar to that of pure PEO with small differences that can be ascribed of differences in nucleation mechanism. Nevertheless, in the samples containing 30% by weight of PEO, the polymer chains of this component are highly confined between PVDF crystals in regions small enough to prevent PEO crystallization. In fact, only between 5 and 8 % of the PEO contained in the sample crystallize in isothermal experiments while in the case of pure PEO crystalline fraction is around 60%. Crystallization kinetics of the part of PEO that crystallizes is much slower than in pure PEO (as seen in isothermal or non-isothermal experiments) and crystal size diminishes as proven by the subsequent melting temperature. Avrami coefficients are much smaller than in pure PEO as well indicating crystal growth of lower dimensionality. Fitting of non-isothermal crystallization using Avrami equation and assuming additivity also shows a significant decrease of the Avrami exponent with confinement in addition to changes in the parameters that determine the temperature dependence of the rate constant. Melting and recrystallization of PVDF in the sample reorganize the PEO phase diminishing the confinement effect on PEO crystallization.

REFERENCES AND NOTES

1. R. M. Michell, I. Blaszczyk-Lezak, C. Mijangos, A. J. Müller. Polymer 2013, 54, 4059-4077.

2. R. M. Michell, A. J. Müller. Progress in Polymer Science 2016, 54–55, 183-213.

3. J. M. Schultz. Frontiers of Chemistry in China 2010, 5, 262-276.

4. D. Wang, Z. Zhang, Q. Yuan, Z. Dong, C. Xiao. Journal of Polymer Research 2010, 17, 745-750.

5. H. Wang, J. K. Keum, A. Hiltner, E. Baer. Macromolecules 2010, 43, 3359-3364.

6. H. Wang, J. K. Keum, A. Hiltner, E. Baer, B. Freeman, A. Rozanski, A. Galeski. Science 2009, 323, 757-760

7. C. Lai, R. Ayyer, A. Hiltner, E. Baer. Polymer 2010, 51, 1820-1829

8. Y. Suzuki, H. Duran, M. Steinhart, H.-J. Butt, G. Floudas. Soft Matter 2013, 9, 2621-2628.

9. J. Maiz, J. Martin, C. Mijangos. Langmuir 2012, 28, 12296-12303.

10. P. Pedrosa, J. A. Pomposo, E. Calahorra, M. Cortázar. Polymer 1995, 36, 3889-3897.

11. E. E. Shafee, W. Ueda. European Polymer Journal 2002, 38, 1327-1335.

12. R. P. Pereira, A. M. Rocco. Polymer 2005, 46, 12493-12502.

13. P. Pan, L. Zhao, Y. Inoue. Macromolecular Materials and Engineering 2013, 298, 919-927.

14. Z. Qiu, T. Ikehara, T. Nishi. Polymer 2003, 44, 3101-3106.

15. P. H. Richardson, R. W. Richards, D. J. Blundell, W. A. MacDonald, P. Mills. Polymer 1995, 36, 3059-3069.

16. P. Huang, Y. Guo, R. P. Quirk, J. Ruan, B. Lotz, E. L. Thomas, B. S. Hsiao, C. A. Avila-Orta, I. Sics, S. Z. D. Cheng. Polymer 2006, 47, 5457-5466.

17. P. Samanta, R. Srivastava, B. Nandan, H.-L. Chen. Soft Matter 2017, 13, 1569-1582.

18. L. Sun, L. Zhu, Q. Ge, R. P. Quirk, C. Xue, S. Z. D. Cheng, B. S. Hsiao, C. A. Avila-Orta, I. Sics, M. E. Cantino. Polymer 2004, 45, 2931-2939.

19. L. Zhu, B. R. Mimnaugh, Q. Ge, R. P. Quirk, S. Z. D. Cheng, E. L. Thomas, B. Lotz, B. S. Hsiao, F. Yeh, L. Liu. Polymer 2001, 42, 9121-9131.

20. M. N. Tamaño-Machiavello, C. M. Costa, J. Molina-Mateo, C. Torregrosa-Cabanilles, J. M. Meseguer-Dueñas, S. N. Kalkura, S. Lanceros-Méndez, R. Sabater i Serra, J. L. Gómez Ribelles. Materials Today Communications 2015, 4, 214-221.

21. C. M. Costa, M. N. T. Machiavello, J. L. G. Ribelles, S. Lanceros-Méndez. Journal of Materials Science 2013, 48, 3494-3504.

22. C. M. Costa, J. Nunes-Pereira, L. C. Rodrigues, M. M. Silva, J. L. G. Ribelles, S. Lanceros-Méndez. Electrochimica Acta 2013, 88, 473-476.

23. A. Gören, C. M. Costa, M. N. Tamaño Machiavello, D. Cíntora-Juárez, J. Nunes-Pereira, J. L. Tirado, M. M. Silva, J. L. Gomez Ribelles, S. Lanceros-Méndez. Solid State Ionics 2015, 280, 1-9.

24. M. N. Tamaño-Machiavello, B. Bracke, C. M. Costa, S. Lanceros-Mendez, R.

Sabater i Serra, J. L. Gómez Ribelles. Journal of Polymer Science Part B: Polymer Physics 2016, 54, 672-679.

25. D. M. Correia, C. M. Costa, J. Nunes-Pereira, M. M. Silva, G. Botelho, J. L. G. Ribelles, S. Lanceros-Méndez. Solid State Ionics 2014, 268, Part A, 54-67.

26. M. Mohamadi, H. Garmabi, M. Papila. Macromolecular Research 2016, 24, 698-709.

27. P. Martins, A. C. Lopes, S. Lanceros-Mendez. Progress in Polymer Science 2014, 39, 683-706.

28. J. F. Kim, J. H. Kim, Y. M. Lee, E. Drioli. AIChE Journal 2016, 62, 461-490.

29. C. M. Costa, M. M. Silva, S. Lanceros-Mendez. RSC Advances 2013, 3, 11404-11417.

30. P. Martins, C. M. Costa, J. C. C. Ferreira, S. Lanceros-Mendez. The Journal of Physical Chemistry B 2012, 116, 794-801.

31. A. T. Lorenzo, M. L. Arnal, J. Albuerne, A. J. Müller. Polymer Testing 2007, 26, 222-231.

32. B. Wunderlich. Macromolecular physics; Academic Press, 1973.

33. M. Avrami. The Journal of Chemical Physics 1939, 7, 1103-1112.

34. M. Avrami. The Journal of Chemical Physics 1941, 9, 177-184.

35. J. M. Schultz. Polymer Materials Science; Prentice-Hall, 1974.

36. J. M. Schultz. Polymer Crystallization: The Development of Crystalline Order in Thermoplastic Polymers; American Chemical Society, 2001.

37. J. D. Hoffman, R. L. Miller. Macromolecules 1988, 21, 3038-3051.

38. J. J. Point, J. Rault, J. D. Hoffman, A. J. Kovacs, L. Mandelkern, B. Wunderlich, E. A. DiMarzio, P. G. de Gennes, J. Klein, R. C. Ball, e. all. Faraday Discussions of the Chemical Society 1979, 68, 365-490.

39. N. Hannay. Treatise on Solid State Chemistry: Volume 3 Crystalline and Noncrystalline Solids; Springer US, 2012.

40. V. Sencadas, C. M. Costa, J. L. Gómez Ribelles, S. Lanceros-Mendez. Journal of Materials Science 2010, 45, 1328-1335.

41. F. Fraisse, J.-M. Nedelec, J. P. E. Grolier, M. Baba. Physical Chemistry Chemical Physics 2007, 9, 2137-2141.

42. S. K. Chaurasia, R. K. Singh, S. Chandra. CrystEngComm 2013, 15, 6022-6034.

43. M. Yang, C. Gogos. European Journal of Pharmaceutics and Biopharmaceutics 2013, 85, 889-897.

44. S. Imai, S. Shimono, Y. Fukushima, K. Umezaki, M. Okada, M. Takahashi, H. Matsuda. Thermochimica Acta 1995, 267, 259-268.

45. C. Li, Q. Kong, Q. Fan, Y. Xia. Materials Letters 2005, 59, 773-778.

46. A. Adhikari, K. Lozano. Journal of Polymer Research 2011, 18, 875-880.

47. T. Ozawa. Polymer 1971, 12, 150-158.

48. S. A. Madbouly, B. A. Wolf. Journal of Polymer Science Part B: Polymer Physics 2004, 42, 820-829.

49. X. Kong, X. Yang, G. Li, X. Zhao, E. Zhou, D. Ma. European Polymer Journal 2001, 37, 1855-1862.

50. J. Jin, M. Song, F. Pan. Thermochimica Acta 2007, 456, 25-31.

51. T. Liu, Z. Mo, S. Wang, H. Zhang. Polymer Engineering & Science 1997, 37, 568-575.

52. E. Lee, J.-Y. Hong, G. Ungar, J. Jang. Polymer International 2013, 62, 1112-1122.

53. N. Rahmansyah, C.-T. Lo, C.-M. Syu, C.-L. Lee. Polymer International 2011, 60, 1380-1389.

54. J.-T. Xu, Q. Wang, Z.-Q. Fan. European Polymer Journal 2005, 41, 3011-3017.

55. Y. Long, R. A. Shanks, Z. H. Stachurski. Progress in Polymer Science 1995, 20, 651-701.

56. M. L. Addonizio, E. Martuscelli, C. Silvestre. *Polymer* 1987, *28*, 183-188.

GRAPHICAL ABSTRACT

Maria N. Tamaño Machiavello, Carlos M. Costa, Francisco J. Romero-Colomer, José María Meseguer Dueñas, Senentxu Lanceros-Méndez, José Luís Gomez Ribelles

CRYSTALLIZATION KINETICS OF POLY(ETHYLENE OXIDE) CONFINED IN SEMICRYSTALLINE POLY(VINYLIDENE) FLUORIDE

A water-soluble polymer, PEO and a piezoelectric polymer, PVDF, are two widely polymers used in a wide application spectrum and PVDF / PEO blends are blended forming two interconnected phases. The properties of the PVDF / PEO blends are very dependent on the mixing procedure (which in our case produces the dispersion of PEO in very small domains) and on the crystallinity of both components. The melting and recrystallization of PVDF in the sample reorganized the PEO phase by reducing the confinement effect on the crystallization of PEO.

GRAPHICAL ABSTRACT FIGURE